01 Jan 2004

Characterization of Human Metal ESD Reference Discharge Event and Correlation of Generator Parameters to Failure Levels-Part I: Reference Event

Ramachandran Chundru

David Pommerenke
Missouri University of Science and Technology, davidjp@mst.edu

Kai Wang

Thomas Van Doren
Missouri University of Science and Technology

et. al. For a complete list of authors, see *https://scholarsmine.mst.edu/ele_comeng_facwork/920*

Recommended Citation

Characterization of Human Metal ESD Reference Discharge Event and Correlation of Generator Parameters to Failure Levels—Part I: Reference Event

Ramachandran Chundru, David Pommerenke, Kai Wang, Tom Van Doren, *Fellow, IEEE*, Federico Pio Centola, and Jiu Sheng Huang

Abstract—**Electrostatic discharge (ESD) generators are used for testing the robustness of electronics toward ESD. Most generators are built in accordance with the IEC 61000-4-2 specifications. Using only a few parameters, this standard specifies the peak current, the rise time and the falling edge. Lacking a transient field specification, test results vary depending on which generator is used, even if the currents are quite similar. Such a specification is needed to improve the test repeatability. As for the current, the specification should be based on a reference human metal ESD event. While keeping the presently set peak current and rise time values, such a reference ESD (5 kV, 850-μm arc length) is identified and specifications for current derivative, fields, and induced voltages are derived. The reference event parameters are compared to typical ESD generators.**

Index Terms—**Discharge current, electrostatic discharge (ESD), field sensor, susceptibility, transient fields.**

I. INTRODUCTION

ELECTROSTATIC discharge (ESD) generators are used for testing the robustness of electronics toward ESD. Their aim is to emulate the discharge of a human through a small piece of metal (human metal ESD). For reasons of reproducibility of the test result, i.e., to avoid the influence of the arc length on the discharge current [1]–[5], contact mode discharges are used whenever possible. Here, the spark is confined to a high-voltage relay. Most generators are built in accordance with the specifications spelled out in IEC 61 000-4-2 [6]. As a reference ESD scenario, the discharge of a human through a small piece of metal has been taken. This is called the human metal ESD to delineate it from the HBM-ESD model that is common in device testing. Relative to the HBM-ESD model, the human metal ESD shows much larger currents and faster rise-times, because the human body model (HBM)-ESD model assumes a discharge that originates from the skin.

For contact mode discharges a peak current value of 3.75 A/kV, a rise time of 0.7–1 ns and two current values during the falling edge are specified. The rationale for these specifications is not documented, but publications such as [7]–[9] most likely influenced the committee.

Even though all the generators have peak current values and risetimes very similar to the ones specified in the standard, some of the generators fail the equipment under test (EUT) at vastly different voltage levels from the others. A range of 1 : 5 is shown in the second part of this two-paper series. This indicates that even though all the generators are made in accordance with the above-mentioned standard they produce different ESD events leading to a serious repeatability problem when the same EUT is tested with different brand generators. The problems have been well documented although the connection between parameters and EUT failures has been speculative so far [10]–[15]. These previous studies were generally unsuccessful in correlating well-performed parametric characterization (at bandwidths exceeding 1 GHz) with ESD failure levels on tested electronic systems.

This work derived a reference ESD discharge event that is based on actual human metal ESD. Its current, current derivative, and field parameters are given. The objective of this reference event is to provide guidance for designing an optimal ESD generator and to provide excitation information for studies on susceptibility and shielding.

The voltage induced in a small loop is introduced as a parameter for characterizing ESD generators. As shown in the second article of this series, the induced voltage correlates well with observed EUT failure levels for those EUT's having failure levels that are strongly affected by the ESD chosen generator. Including this parameter into the standard would offer distinctive advantages over the direct measurement of transient field, e.g., the suppression of low-frequency components, a well reproducible frequency response up to many gigahertz, and its broad availability due to its very simple construction.

By comparing fields and currents, Section I shows that both need to be specified in an ESD standard. Section II explains the measurement setup and Section III gives details of the reference ESD event.
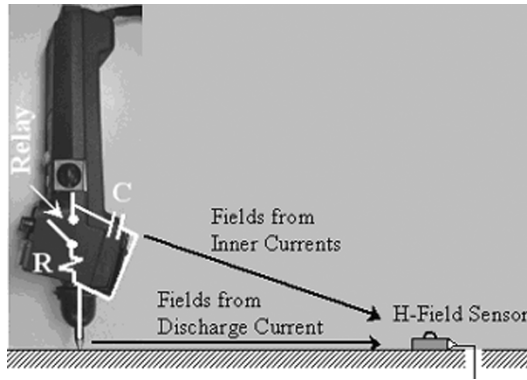
Fig. 1. Sideview and coarse equivalent circuit of the ESD generator to illustrate the two dominating causes for the related magnetic field.
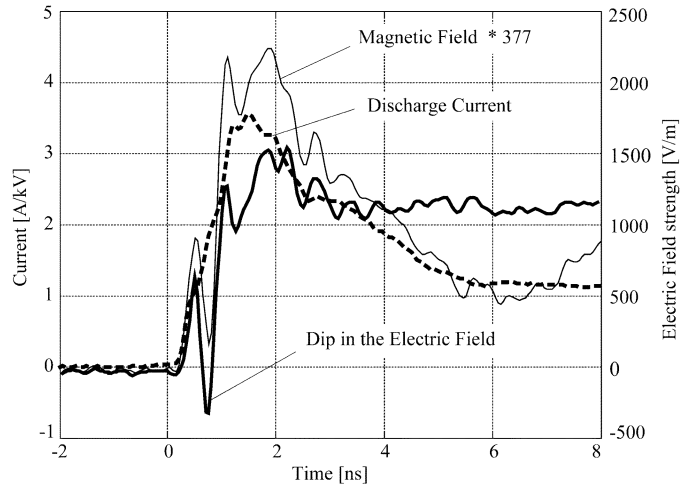

Fig. 2. Solid waveform is the electric field strength of an ESD generator normalized to 1 kV, measured at a distance of 10 cm from the discharge point. Also shown is the magnetic field strength multiplied by the intrinsic impedance of free space for reasons of scaling.

II. RELATIONSHIP BETWEEN ESD CURRENT AND FIELD WAVEFORM

At first thought, it is convincing to assume that a smooth current waveform will yield a smooth transition of the electromagnetic fields. If this holds true, it would be sufficient to regulate the discharge current alone. The present rise time limit, amended by a maximal current derivative, would ensure a smooth current rise. An additional limit to the negative current derivative would prevent the current from falling too fast after the initial rise and limit the amount of ringing on the current. If the assumption holds true, just enforcing a smooth current waveform at the point of injection could minimize the dependence of ESD test results in contact mode on the ESD generator used.

The relationship between discharge current and fields is much more complex than the above assumption suggests. It works best when the magnetic field is measured very close to the discharge tip. Within a few centimeters, the field is governed by Ampere's law and can be estimated from the discharge current. However, with increasing distance from the discharge point, the magnetic field will also be determined by the current distribution on the complete ESD generator structure and its ground strap (Fig. 1), not only by the current at the discharge point as often mistakenly assumed. While the discharge current may vary smoothly and may show a rise time of 0.7–1 ns, other current components within the generator will rise much faster. In contact mode, ESD the discharge is initiated within a relay. Often pressurized $N_2 + SF_6$ (sulfur-hexafloride) relays are used. The voltage collapse across the contacts is hard to measure given data from ESD generators having no pulse forming network. This article and applications of these relays in transmission line pulsers [16] suggest that the voltage collapses in less than 100 ps.

As an example of this effect, the current and the fields of an ESD generator are shown in Fig. 2. The current rises smoothly, but the electric and magnetic fields have a strong dip.

For pulse forming, this ESD generator uses a folded back capacitor. It is constructed from copper foil and resistors and increases the rise time of the current as measured at the discharge tip (Fig. 1). This R-C structure includes the relay and forms a rather large loop. Within this loop fast rising currents are flowing. Upon closing of the relay, transient fields that are not directly related to the current at the discharge tip will be radiated.
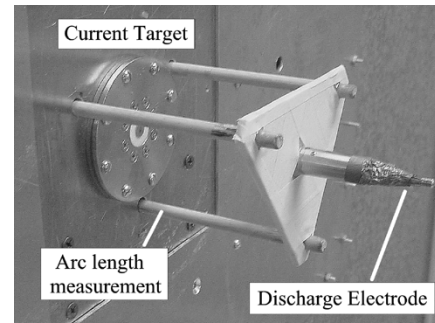

Fig. 3. Current Target, part of the arc length measurement system and discharge electrode. The hand-held metallic discharge electrode is the air discharge electrode of a Minizap MZ-15 ESD generator. Its internal resistor was shorted.

Most other generators acted in a similar fashion. This shows that the simplified assumption stated at the beginning of this section cannot be used, i.e., the fields or related properties need to be specified in addition to a current specification to improve the test result uncertainty.

III. MEASUREMENT SETUP

The measurement setup needs to capture the discharge current, transient fields, the arc length for human metal ESD, and the voltages induced in a small loop. The wall of a shielded room was used as a ground plane having current and field sensors placed upon it while the instrumentation was placed inside. For the measurement of human metal ESD, the person held a metallic discharge electrode in his hand (Fig. 3). The person was charged, in most experiments to 5 kV via a 100-MΩ resistor. Then, as the person moved the electrode toward the current target, a discharge occurred.

The current is initiated by the spark breakdown of the gap between the metallic discharge electrode and the ground plane. Current, the gap distance at the moment of the breakdown (i.e., the arc length), transient fields using broad-band field sensors [17] and induced voltages are measured.
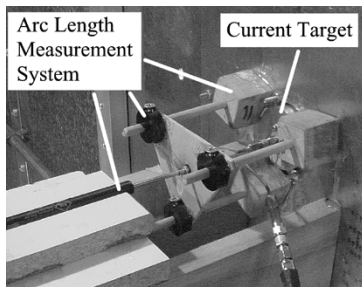
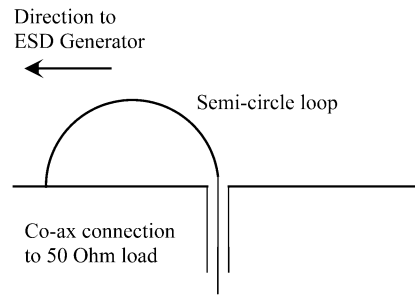Fig. 4. Arc length measurement setup (back side).

Fig. 5. Semicircle loops on the ground plane having a radii of 14 mm and 5 mm were used. The wire diameter was 0.7 mm. The loops were placed at distances of 0.1 or 0.4 m from the current target center. The loops were loaded with 50 Ω and were not shielded.

A. Oscilloscope

Three different oscilloscopes recorded the measurements.

1) HP Infinium oscilloscope (1.5 GHz, 8 GS/s) to measure the discharge current.
2) Tektronix TDS7404 oscilloscope (single channel, 4 GHz, 20 GS/s) to measure the transient fields.
3) Wavemaster 8500 Lecroy oscilloscope (dual channel, 5 GHz, 20 GS/s) for measuring most of the induced voltage data sets.

B. Current Target

Due to insufficiencies of the Pelligrini target [15], [18]–[20] for measurements above 1 GHz, an improved current target was used. Its frequency response is within ± 0.3 dB up to 1 GHz and ± 0.8 dB up to 4 GHz.

C. Arc Length Measurement

The discharge electrode is moved toward the current target at speeds of about 0.01–1 m/s. The gap distance is measured using a precision position sensor (black part to the left in Fig. 4). At the moment of discharge, the momentary value of the gap-distance is stored in a Track and Hold. The arc length measurement is accurate within $\pm 50\ \mu$m within the speed range used.

D. Semicircle Loop Sensors

A limited number of laboratories are able to conduct transient field measurement having a large useful time window (broadband flat frequency response). For that reason it may be difficult to require such measurements in an ESD standard. An alternative is to measure the voltage induced in a ground plane mounted semi-loop of given size having a given termination resistance, as shown in Fig. 5. Such a measurement offers additional advantages.

1) Due to the transfer function (predominantly H-field to voltage at the load) low-frequency components are suppressed. This improves the achievable dynamic range for the high-frequency components. Otherwise, the dynamic range of nominal 8-bit oscilloscopes limits the ability to measure high-frequency components, as the vertical scaling is determined by low-frequency components. The high-frequency components are then often covered by the quantization noise and possibly artifacts from A/D converter misalignment. The ability to improve S/N ratio, using averaging in the time domain is limited due to limited pulse-to-pulse repeatability at high frequencies,

possibly resulting from spark initiation within a relay. Without careful attention to pulse-to-pulse repeatability and trigger point jitter, time domain averaging may act as a low-pass filter.

2) The voltage induced in a small loop follows the intuition of the coupling process. One can associate an equivalent loop area for each connector, trace or socket, and obtain an estimate of the induced voltage from this data. Probably without having beyond 1-GHz frequencies in mind, this has been proposed for ESD induced errors by Mardiguian [21].
3) The frequency response of the field sensors used in our lab is limited to 2 GHz, while the frequency response of a loop can be characterized from its mechanical dimensions up to much higher frequencies.
4) The voltage induced in such a small loop correlates well to failure levels (soft-errors) in fast CMOS devices, as shown in the second article.

The overall test setup, configured for the measurement of human metal ESD, allows capturing:

- discharge current at 8 GS/s sampling rate and up to 1.5-GHz bandwidth, instead, if the TDS 7404 is used, this would have been at 20-GS/s sampling rate and up to 4-GHz bandwidth;
- transient H-field on the surface of the ground plane up to 2 GHz;
- transient E-field up to 2 GHz, when the H-filed sensor is replaced by the E-field sensor;
- gap distance at the moment of discharge.

By replacing the field sensor with the semi-loop, the same setup is used to capture the induced voltages. For some datasets a LeCroy 8500 oscilloscope allowed the recording of two channels at 5-GHz bandwidth and 20 GS/s simultaneously.

IV. ESD REFERENCE EVENT

A. Arc Length Influence on the Discharge Current Waveform

The objective of the ESD standard is to reproduce the stress level of ESDs as they might be experienced by electronic systems. There are a wide variety of possible ESD events, e.g., the discharge of furniture, human discharge via a small metal piece or via the skin, discharges of a cable while it is connected, often called "charged cable event (CCE)." For each event, the severity is dependent on the voltage and the arc length [1], [2], [4], [22],
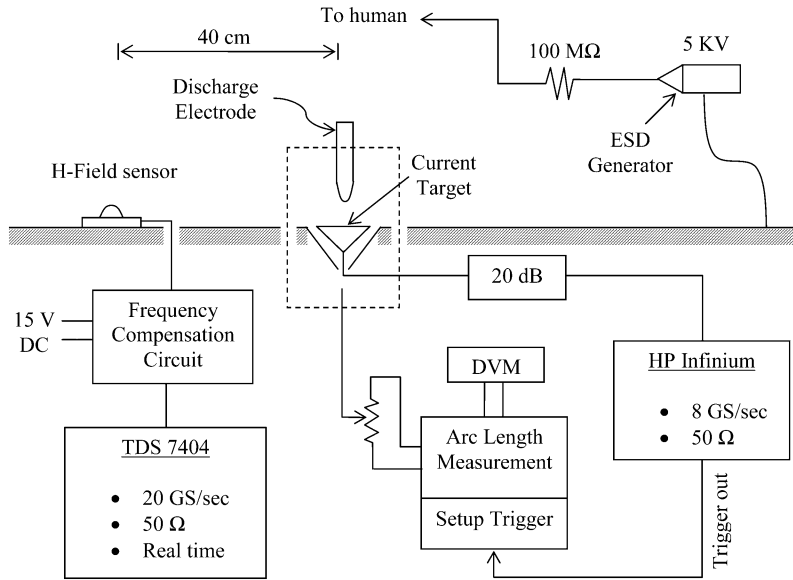
Fig. 6.   Overall setup for measuring human metal ESD currents, arc lengths, and fields.
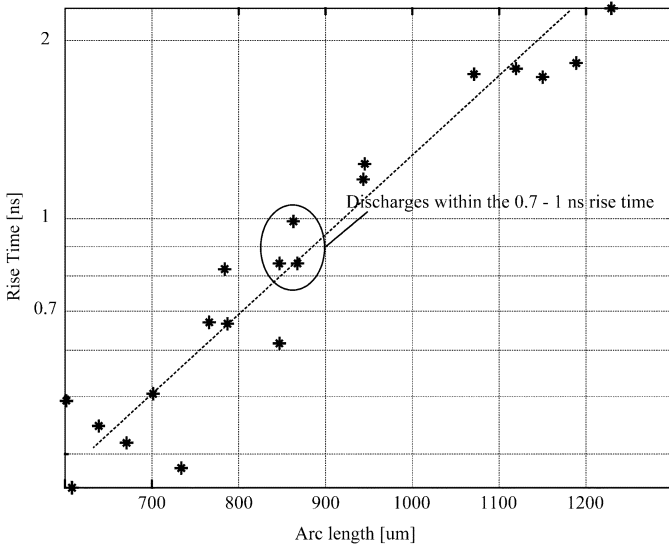

Fig. 7.   Rise time as a function of arc length for human metal ESDs at 5 kV.
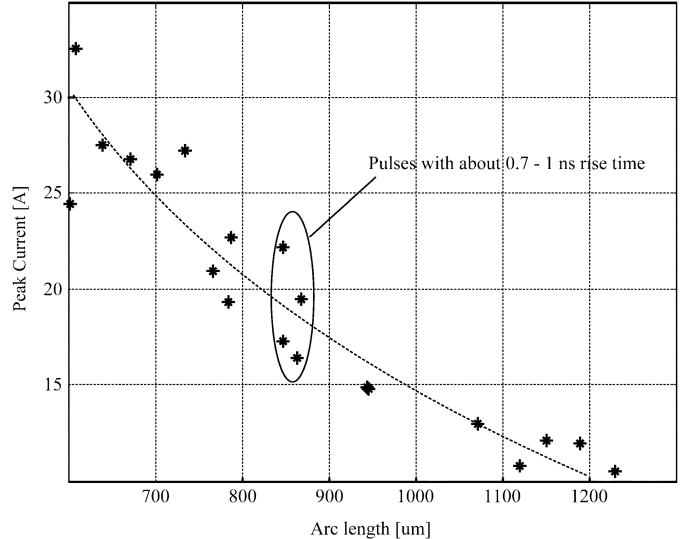

Fig. 8.   Peak current as a function of arc length for human metal ESDs at 5 kV.

[23]. If a human or an object is charged to the same voltage and discharged repeatedly, a large variation of current waveforms will be observed. This has been often incorrectly attributed to corona and attempts have been made to correlate rise time to the curvature of the ESD generator tip. However, the variations in the current are a result of differences in arc length. A typical example is shown in Fig. 7 for the rise time and in Fig. 8 for the peak current. Further data can be found in [1], [4], and [23]. The shorter the arc length, the larger the peak current, and the faster the initial current rise will be.

It has been shown that the rise time may be as low as 50 ps for discharges above 1.5 kV [5], and faster for lower voltages or at higher air pressure [16]. Within the range of arc lengths observed in the datasets, presented by Figs. 7 and 8, the rise time varied from 600 ps to 1.3 ns. For the lowest peak currents, a value of 10 A was recorded, while the largest currents reached 35 A. For the purpose of defining a reference event, it is not important to maximize the range of arc lengths observed. Instead,

the emphasis is taken on discharges having arc lengths of about 0.85 mm. They show rise times and peak values close to the IEC specifications [6]. For that reason they have been selected as bases for the human metal ESD reference event. A current reference has been derived as mathematical function, while the fields and induced voltages have been obtained using measurements.

A mathematical model for the ESD reference event current is given in [17]. It was differentiated with respect to time as indicated by

$$\text{Current Derivative} = \frac{I_n - (I_{n-1})}{\Delta t}.$$

Current derivatives of the measured human metal ESD events at 5 kV and with arc lengths around 850 μm, were also calculated using the same algorithm.

Both the mathematical model and the measured reference current are smooth, i.e., their current derivatives are not much larger than one would expect in a linear rise and their negative current
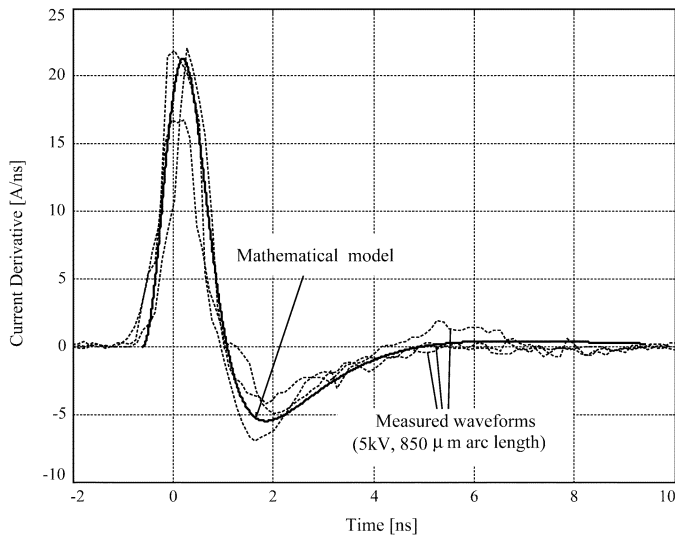
Fig. 9. Current derivatives of measured human metal ESD (5 kV, arc length = 850 μm) and mathematical reference waveform as given in [17].
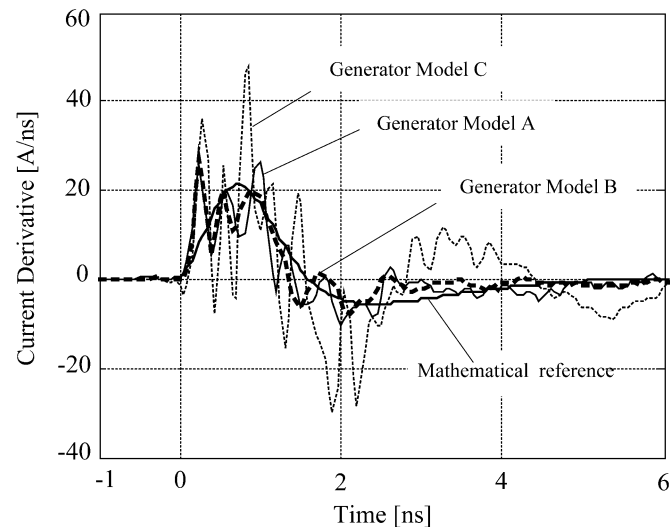

Fig. 10. Current derivatives of different ESD generators relative to the human metal reference event. Generator data is valid for 5 kV contact mode discharge.

derivative values are significantly lower than the positive current derivative values, indicating that the initial current pulse rises rapidly, but falls slowly. Typically, the magnitude ratio of positive to negative current derivatives is larger than $1:3$.

It is interesting how present day ESD generators compare to the current derivative of the reference event. These data are presented in Fig. 10.

Fig. 9 and [17] show how the current and current derivative of the mathematical model compare to those of the measured human metal ESD at 5 kV with arc length around 850 μm. In Fig. 10, the current derivative is compared to three generators. Two of the generators, Models A and B, exhibit a smoothly rising current. In contrast, the current of generator C falls off sharply after the initial peak and rings considerably. The mathematical model yields the parameters shown in Table I.

B. Spectral Density of the Reference Current Waveform

The spectral current densities of the mathematical model and the measured reference events are compared in Fig. 11. The DC

TABLE I
PARAMETERS CALCULATED FROM THE MATHEMATICAL MODEL

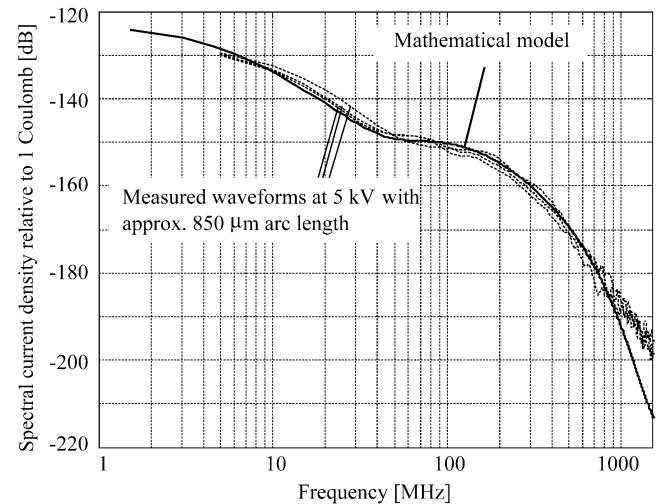| Parameter	Value
Peak current	3.78 A/kV
Rise time	863 ps
Total capacitance	154 pF (150 pF bulk and 4 pF hand capacitance)
Peak positive derivative	4.26 A/(ns kV)
Peak negative derivative	- 1.1 A/(ns kV)

Fig. 11. Spectral distribution of the reference waveform current.

value of the spectral distribution of the current shown in Fig. 11 equals the total charge; the Fourier transform of current yields a unit of ampere per hertz, which is equivalent to ampere per second or coulomb. A 150-pF capacitor charged to 5 kV contains a charge of -122.5dB relative to 1 C. The reference event matches the spectral density of the measured data up to about 1 GHz. Above 1 GHz, the measured data may be influenced by the limited dynamic range of the oscilloscope.

C. Transient Fields of the Reference ESD Event

As explained previously, a smooth current does not always result in smooth transient fields. Thus, it is not sufficient to merely analyze the ESD current. In addition, the fields need to be investigated. Transient fields of the reference event (human metal ESD at 5 kV and with arc lengths around 850 μm) are shown in the following figures. To obtain this data, broad-band field sensors were placed on the ground plane at a distance of 0.4 m from the discharge point.

The electrostatic field cannot be measured by the sensors used, as they have a high pass characteristic, i.e., they show 0 V/m before the discharge begins. The electrostatic field was estimated by offsetting the measured field strength such that 0V/m is obtained 2 00 ns after the beginning of the discharge. This yields an electrostatic field of about 4000 V/m at 0.4 m distance and 5 kV charging voltage.

The electric field strength of human metal ESD reference events are shown in Fig. 12. Due to slight variations in hand position, the initial electrostatic field varies around -4000 V/m. For the magnetic field it is worthwhile to test insofar as the field strength can be estimated using Ampere's law, although the distance is already 0.4 m. If, for example, a 5-kV discharge having
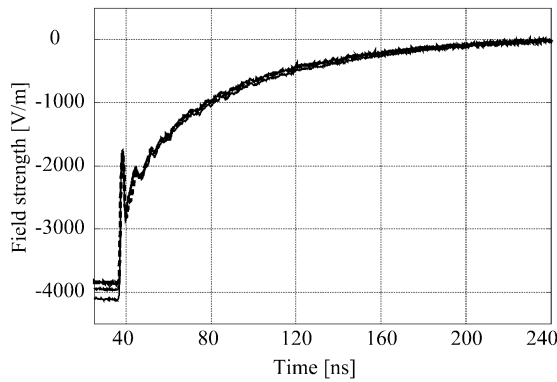
Fig. 12. Electric field strengths of three human metal discharges at 5 kV with arc lengths of around 850 μm, 0.4-m distance.
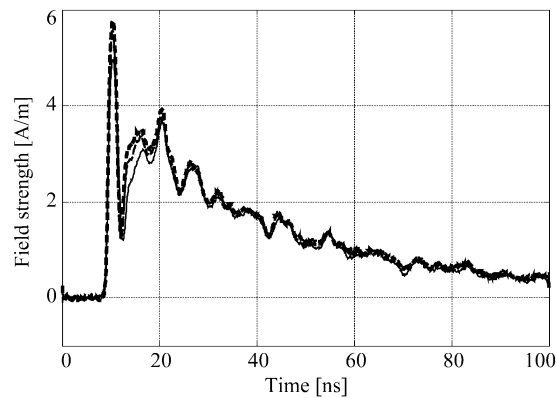

Fig. 13. Magnetic field strength of three human metal discharges at 5 kV with arc lengths of around 850 μm. The field strength was measured at a distance of 0.4 m, deconvolved for correcting the low-frequency roll-off of the sensors and low-pass filtered with a cutoff frequency of 2 GHz.

a 20-A peak current is considered, a field strength of 8 A/m is obtained using Ampere's law

$$H = \frac{I}{2\pi r}$$
$$H = \frac{20 \text{ A}}{2\pi x 0.4 \text{ m}} \cong 8 \frac{\text{A}}{\text{m}}.$$

This estimation assumes a current that flows for an infinite distance and with no displacement current return between the sensor and the metallic part. Still, it provides a general check for the validity of the test results. It can be observed from Fig. 13 that the measured field strengths were close to the theoretical values as obtained using Ampere's law. The overall H-field strength decay with distance on the ground plane can be approximated by $1/r$ for small and larger distances. A more detailed discussion on the distance dependence is given in [3].

D. Voltages Induced in a Small Loop by the Reference ESD Event

The voltage induced in a small loop is closely related to the transient fields. The loop couples predominately to the magnetic field. As discussed in Section II, the voltage induced in a loop is a simple and effective method characterizing these transient fields without directly measuring the transient fields. This measurement will show if fast changing currents within the generator, which often do not reach the discharge tip, are causing high-frequency components of the transient fields that
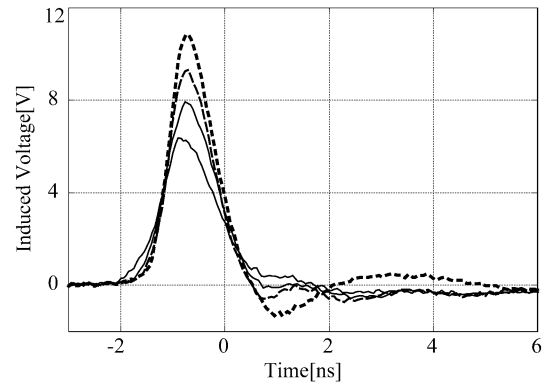

Fig. 14. Voltages induced in a semi-circular loop of 28 mm diameter at a distance of 0.1 m for human metal ESD (5 kV, arc length = 850 μm). The semiloop is loaded with 50 Ω.

overwhelm the fields of the reference event. Voltages induced in a semicircle loop (28-mm diameter) by reference human metal ESDs are shown in Fig. 14, data that compares this to real generators and to EUT failure levels will be presented in the second article of this two-article series.

V. CONCLUSION

The beginning of this article series derived a reference of a ESD event for human metal ESD for measured discharges. It is characterized by current, current derivative, fields, and induced voltages. This information can be used as input for numerical simulation of susceptibility or shielding and it can be used as guidelines for the design of ESD generators. At last, it needs to be pointed out that the main parameters (rise time and peak value) have been chosen such that a new edition of the standard matches the present standard in this respect. In reality, faster rising ESD are likely to happen at lower voltages or in dry conditions at voltages larger than 5 kV. An ESD standard based on this reference event does not intend to provide a 100% ESD failure protection. But due to the broad scope of the IEC 61 000-4-x series of standards this should not be intended. Instead, for specific products or application different reference events can be derived using the descriptive parameters and the methodology shown here.

The second article will discuss the correlation of ESD generator parameters to EUT ESD failure levels, and the consequences of aligning an ESD standard with the suggestions of this paper, with respect to reproducibility and test severity.

REFERENCES

[1] D. Pommerenke, "On the Influence of the Speed of Approach, Humidity and Arc Length on ESD Breakdown," in *ESD Forum*, 1993/1994, pp. 103–111.
[2] B. Daout, H. Ryser, A. Germond, and P. Zweiacker, "The correlation of rising slope and speed of approach in ESD testing," in *Proc. Int. Zurich Symp. Electromagnetic Compatibility*, Zurich, Switzerland, Mar. 1987.
[3] D. Pommerenke, "ESD: What has been achieved, what is less well understood?," in *Proc. 13th Int. Zurich Symp. Technical Exhibition Electromagnetic Compatibility*, Zurich, Switzerland, Feb. 1999, pp. 77–82.
[4] ——, "ESD—Transient fields, Arc simulation and rise time limit," *J. Electrostat.*, vol. 36, no. 1, pp. 31–54, Nov. 1995.

[5] D. Pommerenke and M. Aidam, "ESD: Waveform calculation, field and current of human and simulator ESD," *J. Electrostat.*, vol. 38, no. 1–2, pp. 33–51, Oct. 1996.

[6] *Electromagnetic Compatibility (EMC)—Part 4-2: Testing and Measurement Techniques—Electrostatic Discharge Immunity Test*, 61000-4-2, EN 61000-4-2, 1995.

[7] P. Richman, "Classification of ESD hand/metal current waves versus approach speed, voltage, electrode geometry and humidity," in *Proc. IEEE Int. Symp. Electromagnetic Compatibility*, 1986, pp. 451–458.

[8] ——, "Progress report on a different kind of ESD standard," in *Proc. Int. Zurich Symp. Electromagnetic Compatibility*, 1989, pp. 349–354.

[9] W. M. King and D. Reynolds, "Personnel electrostatic discharge: Impulse waveforms resulting from ESD of human directly and through small hand-held metallic objects intervening in the discharge path," in *Proc. IEEE Int. Symp. Electromagnetic Compatibility*, 1981, pp. 577–590.

[10] J. Maas and W. Rhoades, "New ANSI ESD standard overcoming the deficiencies of world wide ESD standards," in *Proc. IEEE Int. Symp. Electromagnetic Compatibility*, vol. 2, 1998, pp. 1078–1082.

[11] J. S. Maas and D. J. Pratt, "A study of the repeatability of electrostatic discharge simulators," in *Proc. IEEE Int. Symp. Electromagnetic Compatibility*, 1990, pp. 265–269.

[12] H. Hyatt, "The impact of voluntary vs. legal ESD standards," in *Int. J. Electromagn. Compat.*, 1996, vol. 276, pp. 75–82.

[13] K. Hall, "Tests with different IEC 801.2 simulators have different results," in *Proc. EOS/ESD Symp.*, Las Vegas, NV, Sept. 1994, pp. 161–163.

[14] K. Hall, D. McCarthy, D. Dale, D. Smith, J. Nuebel, J. Barth, and H. Hyatt, "Steps taken to determine why different IEC 61000-4-2 ESD generators produce different results," in *Proc. Int. Zurich Symp. Electromagnetic Compatibility*, 1997, pp. 105–108.

[15] J. Barth, D. Dale, K. Hall, H. Hyatt, D. McCarthy, J. Nuebel, and D. Smith, "Measurements of ESD HBM events, simulator radiation and other characteristics toward creating a more repeatable simulation or; simulators should simulate," in *Proc. EOS/ESD Symp.*, 1996, pp. 211–222.

[16] S. Bonisch, D. Pommerenke, and W. Kalkner, "Broadband measurement of ESD rise times to distinguish between different discharge mechanisms," *J. Electrostat.*, vol. 56, no. 3, pp. 363–383, Oct. 2002.

[17] K. Wang, D. Pommerenke, and R. Chundru, "Numerical modeling of electrostatic discharge generators," *IEEE Trans. Electromagn. Compat.*, vol. 45, pp. 258–271, May 2003.

[18] J. Sroka, "Insertion loss as transfer coefficient for the calibration of ESD generators. Is it sufficient to cope with?," in *Proc. IEEE Int. Symp. Electromagnetic Compatibility*, vol. 2, 2001, pp. 838–840.

[19] ——, "Contribution of the target in the measurement uncertainty by calibration of the ESD generator," in *Proc. 14th Int. Zurich Symp. Electromagnetic Compatibility*, Feb. 2001, pp. 189–192.

[20] W. G. Traa, "Approach to improve ESD-generator calibration and the realization of a simple discharge device for very wide band measurements," in *Proc. Int. Symp. Electromagnetic Compatibility*, Zurich, Switzerland, 2001.

[21] M. Mardiguian, *Electrostatic Discharge: Understand, Simulate and Fix ESD Problems*. Warrenton, VA: Don White Consultants, 1986.

[22] B. Daout and H. Ryser, "The reproducibility of the rising slope in ESD testing," in *Proc. IEEE Int. Symp. Electromagnetic Compatibility*, 1986, pp. 467–474.

[23] R. Jobava, D. Pommerenke, D. Karkashadze, P. Shubitidze, R. Zaridze, S. Frei, and M. Aidam, "Computer simulation of ESD from voluminous objects compared to transient fields of humans," *IEEE Trans. Electromagne. Compat.*, vol. 42, pp. 54–65, Feb. 2000.

David Pommerenke was born April 11, 1962 in Ann Arbor, MI. He received the Diploma in electrical engineering and the Ph.D. degree in transient Fields of ESD from the Technical University Berlin, Germany, in 1989 and 1995, respectively.

In 1989, he was with the Technical University Berlin as a Research and Teaching Aassistant in electromagnetic compatibility (EMC) and high voltage. In 1996, he joined Hewlett Packard (HP) and in 2001, he became an Associate Professor with the Electromagnetic Compatibility Group, University of Missouri-Rolla. His areas of research interest are EMC , electrostatic discharge (ESD), numerical calculation, high-voltage partial discharge detection systems, electronics, and design of test and measurement equipment. As relevant to the ESD work, he is a member of IEC TC77b WG-9, the working group that sets the IEC 61 000-4-2 ESD test standard.
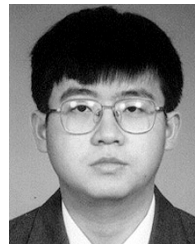
Kai Wang received the B.S. and M.S. degrees in electrical engineering from Tsinghua University, Beijing, China, in 1998 and 2000, respectively. He is currently working toward the Ph.D. degree at the Electromagnetic Compatibility Laboratory, University of Missouri-Rolla, under the direction of Dr. Pommerenke.

His research interests include numerical and experiential study of electrostatic discharge and signal integrity problems, as well as advanced RF measurement.

Tom Van Doren (S'60–M'69–SM'96–F'02) is a Professor of electrical and computer engineering, University of Missouri-Rolla. His teaching and research has focused on electromagnetic compatibility for the past 25 years.

Federico Pio Centola received the Laurea degree in electrical engineering from the University of L'Aquila, L'Aquila, Italy, in 2001, and the M.S. degree in electric engineering from the University of Missouri-Rolla in 2003.

From 2001 to 2003, he was with the Electromagnetic Compatibility Laboratory, University of Missouri-Rolla. In 2003, he joined Flomerics Inc., Santa Clara, CA, as an Electromagnetic Application Engineer.

Ramachandran Chundru was born in India in 1977. He received the B.S.E.E. degree from the University of Madras, Madras, India, in 2000 and the M.S.Comp.E. degree from the University of Missouri-Rolla, in 2001, where he is currently pursuing the M.S.E.E. degree.

Since 2001, he has been studying and working in the Electromagnetic Compatibility Laboratory, University of Missouri-Rolla. His research interests include electrostatic discharge (ESD), electromagnetic compatibility (EMC), signal integrity, high-voltage systems, as well as advanced RF Measurements.

Jiu Sheng Huang received the M.S. degree from the Applied Physics Department, Beijing Institute of Technology (BIT), Beijing, China, and the Ph.D. degree from the Department Electrical Engineering, China M&E College.

He is currently with the Beijing Electrostatic Discharge (ESD) Research Institute, China. His research interests include ESD, electromagnetic compatibility (EMC), and EMI problems in industry, applied electrostatics (AES) and electrostatic instrumentation, and effects of electromagnetic pulse (EMP) on the electronic circuits.